ELSEVIER

Materials Science and Engineering A 427 (2006) 92–98

MATERIALS SCIENCE & ENGINEERING A

www.elsevier.com/locate/msea

Reconstruction and visualization of complex 3D pore morphologies in a high-pressure die-cast magnesium alloy

S.G. Lee, A.M. Gokhale *, A. Sreeranganathan

School of Materials Science and Engineering, Georgia Institute of Technology, Atlanta, GA 30332-0245, United States

Received 13 May 2005; accepted 14 April 2006

Abstract

Visualization and representation of three-dimensional (3D) pore morphologies in the high-pressure die-cast Mg alloys are of significant interest for understanding and modeling processing–microstructure–properties relationships. In this contribution, an efficient and unbiased montage serial sectioning technique is applied for reconstruction of large volume ($\sim 1.24 \times 10^9$ μm^3) high-resolution (~ 1 μm) 3D microstructure of a high-pressure die-cast AM50 Mg alloy containing gas (air) and shrinkage pores. The reconstruction of 3D microstructure from montage serial sections enables visualization and characterization of detailed 3D morphologies and spatial correlations of gas (air) and shrinkage pores. The reconstructed 3D microstructure is implemented in a 3D finite elements (FE) computational framework to illustrate how realistic complex microstructural feature morphologies can be incorporated in the simulations of micromechanical response of these high-pressure die-cast cast microstructures.

Keywords: AM50; Magnesium alloys; Porosity; Three-dimensional microstructure; Finite elements based simulations

1. Introduction

During the recent years, cast magnesium alloys have received considerable attention from the automotive industry for the components such as instrument panels, steering wheels, seat frames, doorframes and power train components [1,2] due to potential of fuel efficiencies and lower emission levels. High-pressure die-casting is the preferred manufacturing process for the Mg alloy components used for automotive as well as for numerous other applications. The high-pressure die-casting process often leads to formation of significant amounts of gas (mostly trapped air) and shrinkage microporosity in the Mg alloy castings [3–10], which adversely affect the fracture related mechanical properties (such as ductility, toughness and fatigue resistance) of the cast Mg alloys [6,11–14]. Consequently, reconstruction of 3D micropore distributions and their incorporation in the property models is of considerable practical relevance. Depending on the material chemistry, processing and microstructural length scales of interest, a 3D microstructure can be rendered using numerous techniques including X-ray computed tomography, magnetic resonance imaging (MRI) and serial sectioning. This contribution concerns visualization of 3D morphologies and connectivity of two types of pores, namely gas (air) and shrinkage pores, present in the cast microstructure of a high-pressure die-cast Mg alloy. The serial sectioning technique is particularly suitable for this class of microstructures because the gas (air) and shrinkage pore dimensions are at different length scales: the thickness of shrinkage pores (which have crack like morphologies) is on the order of few micrometers, whereas the gas (air) pores have sizes on the order 50 μm and gas (air) and shrinkage pores are often interconnected. Further, spacing between gas pores is on the order of few hundred micrometers. Therefore, a large volume of 3D microstructure needs to be reconstructed and visualized at sufficiently high resolution (~ 1 μm). Further, to study the effects of such porosity distributions on the mechanical response of cast microstructure, it is of interest to incorporate such microstructural segment in finite elements (FE) based computational framework.

Classical serial sectioning technique, which enables reconstruction of a small volume segment of 3D microstructure, was developed in the 1970s [15]. The classical serial sectioning technique has been used in numerous investigations to study 3D microstructures of opaque materials [16–20]. An efficient montage based serial sectioning technique is also available [21–27] that permits generation of significantly large volume ($\sim$few mm^3) of 3D microstructure at a *high resolution* (~ 1 μm).

* Corresponding author. Tel.: +1 404 894 2887; fax: +1 404 894 9140.
E-mail address: arun.gokhale@mse.gatech.edu (A.M. Gokhale).

0921-5093/$ – see front matter © 2006 Elsevier B.V. All rights reserved.
doi:10.1016/j.msea.2006.04.095

Table 1
Nominal chemical composition of AM50 alloy

Element	Al	Mn	Zn	Si	Cu	Ni	Fe	Balance
Composition (wt.%)	4.5–5.5	0.25 minimum	0.22 maximum	0.1 maximum	0.01 maximum	0.002 maximum	0.005 maximum	Mg

For approximately the same metallographic effort, the montage based serial sectioning yields microstructural volume containing large number of pores/grains, which can provide sufficiently large statistical sample for study of topological aspects of microstructure such as feature connectivity. Recently, the montage serial sectioning has been implemented in a completely *automated* serial sectioning set-up that utilizes a robotic arm to move the specimen back and forth between the metallographic equipment (polishing, etching, etc.) and optical microscope to generate the montage serial sections in a completely automated manner [27]. In this contribution, the montage serial sectioning technique is applied for reconstruction and visualization of porosity distributions in the high-pressure die-cast Mg alloy. The 3D morphologies and connectivity of gas (air) and shrinkage pores is studied. The utility of the reconstructed 3D microstructure for computational modeling is illustrated by incorporating the 3D digital images of the pores in the finite elements framework for computation of local stress and strain distributions.

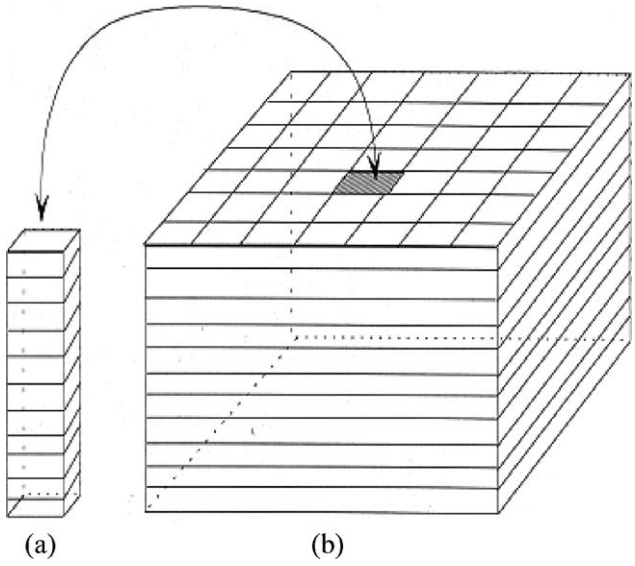

Fig. 1. (a) Small microstructural volume element constructed from a stack consisting of one field of view in each serial section and (b) large volume of microstructure obtained from contiguous small volumes such as those in (a) or by using montage serial sectioning.

2. Experimental

2.1. Materials and processes

The experiments were performed on high-pressure die-cast AM50 Mg alloy having the nominal composition given in Table 1. The square plates of 146 mm × 146 mm × 14.3 mm dimensions were high-pressure die-cast in a cold chamber machine at Gibbs Die Casting Co. The die was heated through passage of steam. The high-pressure die-casting was carried out at the gate velocity of 55 m/s and the melt temperature equal to 705 °C. Intensification pressure was not applied during the die-casting process.

2.2. Metallography

The metallographic specimens were mounted in standard metallographic mounts, and then they were ground using 320–1000-grit abrasive SiC papers. Immediately after the last grinding step, the specimens were washed with water, rinsed with methanol and dried. The fine polishing was conducted using 6 and 1 μm oil based diamond compounds. The final steps in polishing involved the use of 0.3 μm alumina and 0.05 μm colloidal silica. Glycerol and oil base lubricants were used during these polishing steps to avoid the formation of a surface film.

2.3. Montage serial sectioning

To generate a large volume of 3D microstructure at high resolution, one may first reconstruct a small microstructural volume such as the one in Fig. 1a, and then reconstruct many contiguous small volumes surrounding it, perfectly match their boundaries and paste them together to generate a large microstructural volume, as shown in Fig. 1b. A technique equivalent to such a reconstruction has been developed [21,25,26], and in this contribution, it is applied for reconstruction of 3D micropore distributions. First a "montage" of 225 (or more if necessary) contiguous microstructural fields observed at a high magnification (200× for the present microstructure) is created by using the large area high-resolution montage procedure developed by Louis and coworkers [22,28,29]. To create a montage, a field of view (FOV) is arbitrarily chosen in the region of interest in a metallographic plane and the image of this field of view is stored in the memory of image analysis computer as an image file. The right border (of about 60 pixel width) of this image is recalled on the left edge of a blank image. This semi-blank image is then displayed along with the live image. This results in a superimposed image on the left border of the screen (of the previous right border and live image) with rest of the screen having the live image. The automated microscope stage is then programmed to move so that the right border of the live image moves to the left border and gives a reasonable match with the superimposed image. The physical movement of the automatic stage has a large least count and thus cannot achieve perfect match with the previous image. Therefore, image cross-correlation function based technique has been used for automatic pixel-by-pixel matching of the overlapping borders of the two images, which results in a match of the first and the second image with an accuracy of 1 pixel (in the present case, the pixel resolution was 0.5 μm and microscope

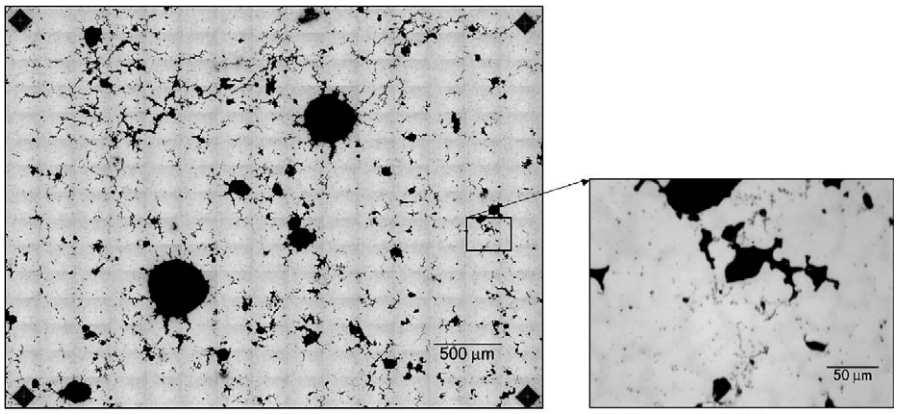

Fig. 2. (a) Montage of 225 fields of view covering an area of 12.4 mm^2 created by matching contiguous microstructural fields grabbed at a resolution of 0.5 μm. The montage is digitally compressed for presentation. Each field of view of the montage has been grabbed at the resolution of the image shown in (b).

resolution was 1 μm). The second image is then stored in the computer memory as another image file. All successive contiguous images are grabbed by using the same procedure and finally a seamless montage of large number contiguous microstructural fields is created. Fig. 2a shows such a montage of 225 fields of view, which has been compressed for display. Each region of this montage has a high resolution of the image shown in Fig. 2b. Therefore, montage is a microstructural image of a large area (∼12.4 mm^2) having a high resolution. In the present work, image analysis was performed on KS-400 image analysis system from Kontron Inc. However, several other commercial image analysis systems also have the required capabilities. The computer codes for creating the montage were written in a language similar to C^{++} in a platform provided by the image analysis software (KS-400).

Once the montage of the first serial section is created and stored in the computer memory, small thickness of the specimen is removed (about 1 μm) by polishing and then a second montage is created at the region exactly below that in the first metallographic plane. In the present study, this polish–montage–polish procedure was repeated to obtain stack of 100 montage serial sections. Microhardness indents were used to locate the exact region of interest in successive serial sections and to measure the distance between consecutive serial sections [21,23]. An important practical problem in the reconstruction of 3D microstructure from serial sections is that the successive serial sections may not be precisely aligned; they may have some transnational and rotational displacement with respect to each other. In the present study, in spite of adjusting the microscope stage, the montages of the consecutive serial sections were often displaced by about ±10 pixels and ±5°, and therefore, it was essential to precisely align successive serial sections. Alignment can be achieved by locating two common points (in the present case, microhardness indents were used for this purpose) in the two consecutive serial sections and translating one image until the first common point is aligned in the two images. Then, the image is rotated about this point until the second common point is also aligned. In the present case, this was accomplished by using 3D image analysis software Voxblast 3.10 in which the images of the montage were digitally translated and rotated until they were exactly aligned to the respective previous sections.

2.4. Reconstruction and visualization of three-dimensional microstructure

The stack of aligned serial sections essentially constitutes a volume image data set similar to those encountered in X-ray computed tomography and magnetic resonance imaging. The steps are involved in the 3D visualization of such data sets are as follows:

- Data generation (in the present case, serial sections);
- Pre-processing such as image alignment, grid regularization, image enhancement and interpolation;
- Rendering of 3D images.

The 3D microstructure visualization can be achieved either by surface rendering or by volume rendering. Surface rendering involves rendering of the iso-surface of the region of interest (ROI) from the volume data, whereas the volume rendering is the rendering of all volume data by specifying opacity and color of each voxel (3D pixel). The surface rendering leads to reduction in the size of the data set because only the surface data are retained. The surface rendering requires fitting of a surface in the volume data. Numerous algorithms are available for surface rendering, including contour connecting algorithm [30] and marching cube algorithm [31]. In the present work, marching cube algorithm has been used for surface rendering of 3D microstructure. In the process of volume rendering, all voxels are visualized by specifying a mapping between rendered image intensity and voxel intensity. In the present work, ray-casting algorithm [32] has been used to for volume rendering of the microstructural images. The 3D image rendering was done by using image analysis software Voxblast 3.10.

3. Results and discussion

In the present work, the 3D microstructure visualization has been done using 100 montage serial sections; each montage

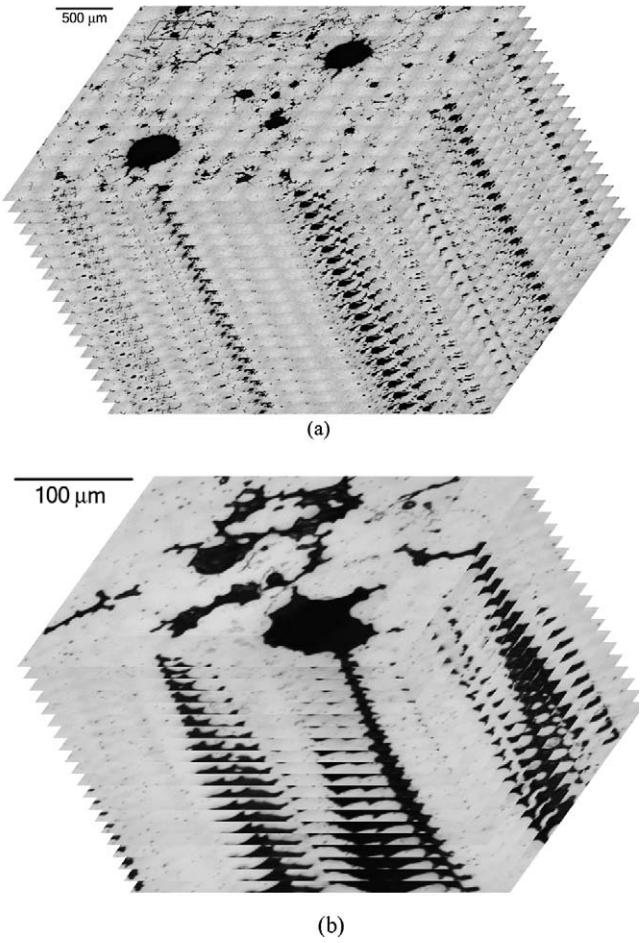

Fig. 3. (a) Stack of 20 montage serial sections for the cast microstructure. Each serial section montage contains 169 contiguous microstructural fields and (b) the magnified view of the small-bordered region of the stack of 20 montage serial sections for the cast microstructure. This is the resolution of the individual microstructural fields.

serial section containing 225 contiguous microstructural fields grabbed at 200×. Therefore, the resulting 3D data sets are useful for characterization and visualization of both short range and long-range spatial dispersion of the micropores.

Fig. 3a shows a stack of aligned 20 montage serial sections for the cast microstructure, where each serial section is a digitally compressed montage of 169 contiguous microstructural fields.[1] Observe that gas pores (equiaxed) and shrinkage pores are interconnected. Focus on the bordered region in Fig. 3a. Fig. 3b is the magnified view of that bordered region, where each section is exactly the stack of serial sections generated by the classical serial sectioning technique [15–20]. This is the magnification at which all microstructural fields have been grabbed. In Fig. 3b, observe the changes in the sizes of the micropores at the edges of these serial sections as well as appearance and disappearance of the smaller pores in the successive serial sections. Fig. 4 shows few segments of volume-rendered 3D microstructure. The

[1] Note that the initial grabbed montages contained 225 contiguous fields, but the borders containing the microhardness indent images were not used for 3D microstructure rendering.

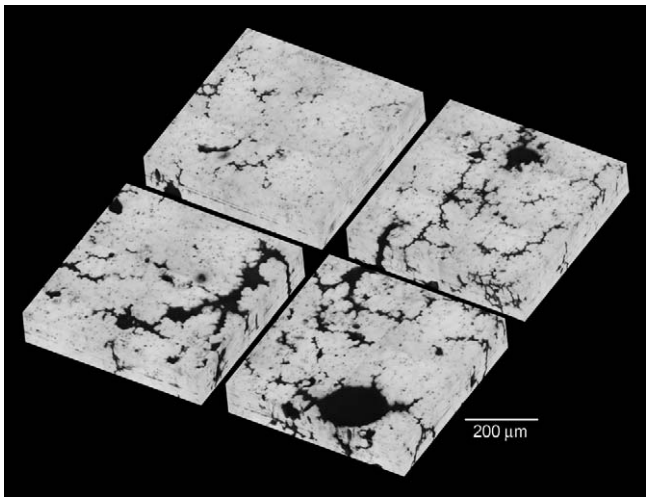

Fig. 4. Small segments of volume-rendered reconstructed 3D microstructure.

volume-rendered visualization is useful for implementation of the 3D microstructural images in the finite elements based computations of the micromechanical response [33]. Fig. 5 shows few segments of surface-rendered 3D microstructure depicting gas and shrinkage pores, whereas Fig. 6 depicts another type of surface rendering of 3D microstructure, where the matrix is effectively removed from the microstructure leaving behind only the pores. Note that the four 3D microstructures displayed in Fig. 5 are only about 8% of the actual 3D microstructural volumes contained in the 100 montage serial sections. These figures clearly show the complexity of the porosity shape and random spatial arrangement of the gas (air) and shrinkage porosity. In this cast microstructure, most of gas (air) and shrinkage pores are connected, except a few that is in very small size ranges. The high-resolution of montage serial sections and large volume permits extraction of individual pores from the 3D microstructure for a more detailed study. Fig. 7a and b display typical individual gas (air) and shrinkage pore morphologies extracted from the 3D microstructure. Fig. 8 displays one of connected poros-

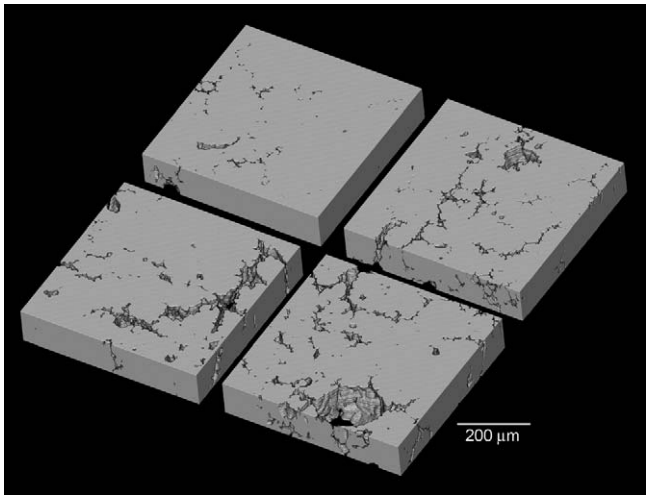

Fig. 5. Small segments of surface-rendered reconstructed 3D microstructure, where the porosity is removed leaving behind just the matrix.

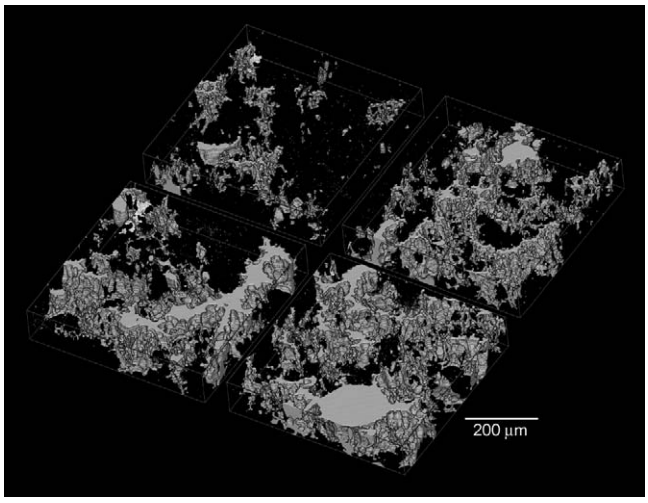

Fig. 6. Small segments of inverted-contrast surface-rendered reconstructed 3D microstructure depicting porosity.

ity. The quantitative measurements reveal that gas (air) porosity in Fig. 7a is on the 90 μm long, average 1066 μm^2 in the cross-sectional area and 95940 μm^3 in volume. Such information on the porosity is extremely useful for understanding the effects of process parameters on the many attributes of porosity and for modeling virtual microstructures and it can be obtained only from large volume high-resolution 3D microstructure generated by a stack of montage serial sections: classical serial sectioning is not useful for this purpose. The complexity of the pore morphologies, spatial connectivity and their spatial arrangement reveal that 2D microstructural observation and/or some quantitative measurements for porosity may seriously underestimate the real three-dimensional porosity size and spatial distribution. Further, some numerical analysis on the mechanical behaviors of the corresponding 2D observational planes can be seriously misleading in that some of fracture related characteristics such as the real three-dimensional stress distribution and preferential crack path cannot be involved in 2D observation planes.

The reconstructed 3D microstructure in STL (stereo lithography) format is exported into Harpoon (CEI), commercial

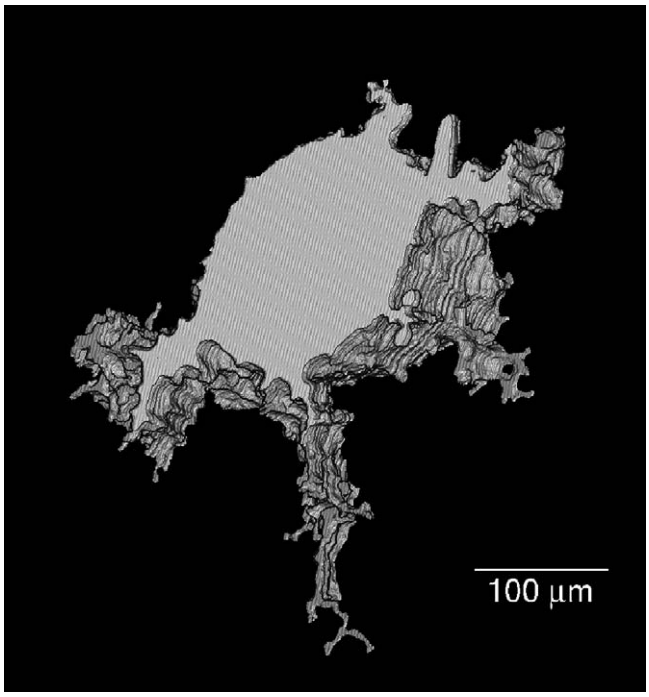

Fig. 8. Three-dimensional morphology of connected porosity extracted from the surface-rendered three-dimensional image.

automatic meshing software to mesh the geometry with tetrahedral elements. Only the external volume of the STL file is meshed leaving the voids (porosity) free of elements. Fig. 9a shows an FE mesh created from a small section (650 μm × 650 μm × 250 μm) of the reconstructed 3D microstructure. The microstructure is embedded in a homogeneous material volume to avoid edge effects. The mesh contains 719329 linear tetrahedral elements and the elements are well refined at the interface as can be observed in the figure. The FE mesh is then exported to ABAQUS, commercial finite element code and analyzed for the elastic mechanical response to a tensile load. Fig. 9b shows the local von Mises stress distribution in the microstructural volume due to a tensile load. Elastic modulus and yield stress of AM50 alloy obtained from experimental tensile test data is used as the constitutive equation in

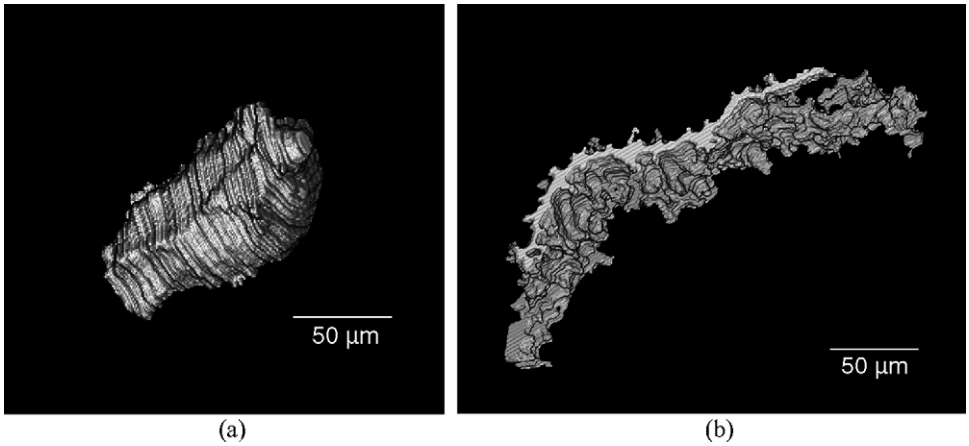

Fig. 7. (a) Three-dimensional morphology of individual gas (air) and (b) shrinkage porosity extracted from the surface-rendered three-dimensional image.

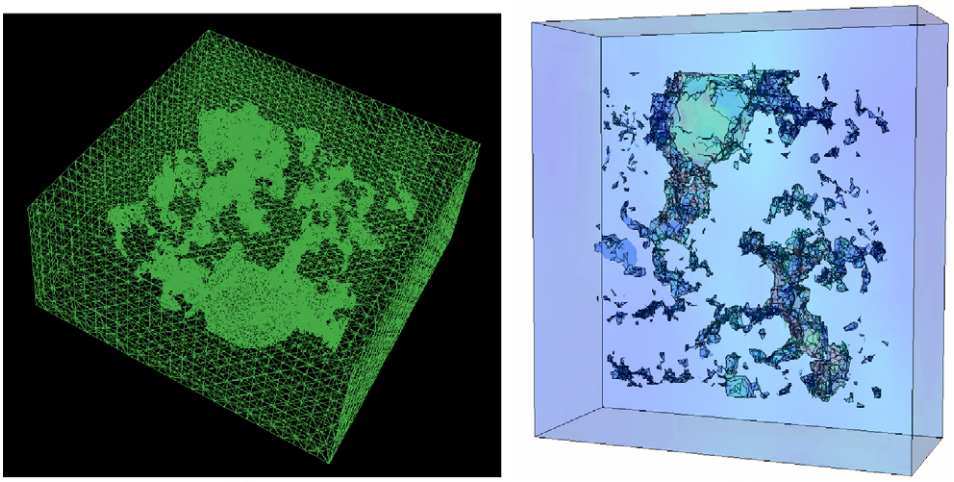

Fig. 9. (a) Three-dimensional finite element mesh and (b) corresponding analysis showing stress distribution around porosity.

the FE model to simulate the elastic response. It must be noted that, in general, the constitutive properties to input in the FE model should be obtained at the microlevel from a region free of porosity (and not from the macroscopic tensile test data) to accurately study the effect of porosity on the mechanical properties of the material. In the present contribution, the FE analysis is presented to illustrate the *methodology* for incorporation of the reconstructed 3D digital microstructural image in the computational framework of the FE techniques and not for reporting the micromechanical response of the 3D microstructure. Such detailed analyses and results will be presented in a separate contribution.

4. Summary and conclusions

A montage serial sectioning technique has been used to generate high-resolution (~1 μm) large volume (1.24×10^9 μm^3) 3D microstructures of micropores in a high-pressure die-cast AM50 Mg alloy. The visualization of the reconstructed 3D microstructure yields the 3D morphologies of the gas (air) and shrinkage pores, their connectivity and spatial correlations. The reconstructed 3D microstructure can serve as a representative volume element in the FE based computational simulations of mechanical response.

Acknowledgements

This research was supported through research grant from U.S. National Science Foundation (NSF grant no. DMR-0404668). Dr. Sreeramamurty Ankem is the Program Managers for the grant. The financial support is gratefully acknowledged. Any opinions, findings and conclusions or recommendations expressed in this contribution are those of the authors and do not necessarily reflect the views of the funding agencies. The authors thank Mr. Kent Misegades, President, CEI, for providing with an evaluation copy of Harpoon.

References

[1] B.L. Mordike, T. Elbert, Mater. Sci. Eng. A302 (2001) 37–45.
[2] B.R. Powell, L.J. Ouiment, J.E. Allison, J.A. Hynes, R.S. Beals, L. Kopka, P.P. Reid, in: A. Luo (Ed.), Proceedings of the Magnesium Technology, TMS, Warrendale, PA, 2004, pp. 3–10.
[3] A. Balasundaram, A.M. Gokhale, Mater. Charact. 46 (2001) 419–426.
[4] A.K. Dahl, S. Sannes, D.H. St. John, H. Westengen, J. Light Met. 1 (2001) 99–103.
[5] B.J. Coultes, J.T. Wood, G. Wang, R. Berkmortel, in: H.I. Kaplan (Ed.), Proceedings of the Magnesium Technology, TMS, Warrendale, 2003, pp. 45–50.
[6] A.M. Gokhale, G.R. Patel, in: J. Hryn (Ed.), Proceedings of the Magnesium Technology, TMS, Warrendale, PA, 2001, pp. 195–199.
[7] Y.J. Huang, B.H. Hu, I. Pinwill, W. Zhou, D.M.R. Taplin, Mater. Manuf. Processes 15 (2000) 97–105.
[8] V.D. Tsoukalas, J. Eng. Manuf. 218 (2004) 77–86.
[9] W.P. Sequeria, M.T. Nurray, G.L. Dunlop, D.H. St. John, Proceedings of the Automotive Alloys, TMS, Warrendale, PA, 1997, pp. 169–187.
[10] D.F. Allsop, D. Kennedy, Pressure Die Casting, The technology of the Casting and the Die, Pergamon Press, Oxford, UK, 1983, pp. 216–219.
[11] A.M. Gokhale, G.R. Patel, in: M. Skillinberg, S. Das (Eds.), Aluminum 2002: Proceedings of TMS Symposium on Automotive Alloys, TMS, Warrendale, 2002, pp. 65–73.
[12] E.M. Gutman, Y.B. Unigovski, A. Eliezer, E. Abramov, E. Aghion, Mater. Technol. 16 (2001) 126–132.
[13] H.T. Gjestland, S. Sannes, H. Westerngen, D. Albright, Die Cast. Eng. (July) (2004) 56–65.
[14] C.-M. Hung, M.-S. Chang, N.-K. Tang, in: A.A. Luo (Ed.), Proceedings of the Magnesium Technology, TMS, Warrendale, PA, 2004, pp. 193–196.
[15] F.N. Rhines, K.R. Craig, Metall. Trans. A 7A (1976) 1729.
[16] R.S. Sidhu, N. Chawla, Mater. Charact. 52 (2004) 225.
[17] M. Li, S. Ghosh, O. Richmond, H. Weiland, T.N. Rouns, Mater. Sci. Eng. A265 (1999) 153.
[18] K.M. Wu, M. Enomoto, Scripta Mater. 46 (2002) 569.
[19] M.V. Kral, M.A. Mangan, G. Spanos, R.O. Rosenberg, Mater. Charact. 45 (2000) 17.
[20] T. Yokomizo, M. Enomoto, G. Spanos, R.O. Rosenberg, Mater. Sci. Eng. 344A (2003) 261.
[21] A. Tewari, A.M. Gokhale, R.M. German, Acta Mater. 47 (1999) 3721.
[22] A.M. Gokhale, A. Tewari, J. Microsc. 200 (2000) 277.
[23] A. Tewari, A.M. Gokhale, Mater. Charact. 46 (2001) 329.

[24] M.D. Dighe, A. Tewari, G.R. Patel, T. Mirabelli, A.M. Gokhale, Trans. Am. Foundry Soc. 99 (2000) 353.
[25] A. Tewari, Ph.D. Dissertation, Georgia Institute of Technology, 1999.
[26] H. Singh, A.M. Gokhale, Mater. Charact. 54 (2005) 21.
[27] J.E. Spowart, H.M. Mullens, B.T. Puchala, J. Met. 55 (10) (2003) 35–37.
[28] P. Louis, A.M. Gokhale, Metall. Mater. Trans. A 26A (1995) 1449.
[29] P. Louis, A.M. Gokhale, Acta Mater. 44 (1996) 1519.
[30] E. Keppel, IBM J. Res. Dev. 19 (1975) 2.
[31] E.W. Lorensen, H.E. Cline, Comput. Graph. 22 (1987) 38.
[32] P. Sabella, Comput. Graph. 22 (1988) 51.
[33] Z. Shan, A.M. Gokhale, Acta Mater. 47 (2001) 3721.